Syntheses, structures, and luminescence of two Zn(II) coordination polymers based on 5-(4-imidazol-1-yl-phenyl)-2H-tetrazole and carboxylates

Yan Xie, Junjie He, Tingting Wang & Heping Zeng

View supplementary material

Accepted author version posted online: 11 Mar 2015.
Published online: 07 Apr 2015.

Submit your article to this journal

Article views: 58

View related articles

View Crossmark data

Taylor & Francis
Taylor & Francis Group

Syntheses, structures, and luminescence of two Zn(II) coordination polymers based on 5-(4-imidazol-1-yl-phenyl)-2H-tetrazole and carboxylates

YAN XIE*†‡, JUNJIE HE†, TINGTING WANG† and HEPING ZENG*†

†Institute of Functional Molecule, School of Chemistry and Chemical Engineering and the Key Laboratory of Fuel Cell Technology of Guangdong Province, South China University of Technology, Guangzhou, PR China
‡Department of Chemical Engineering, Chemical Engineering Research Center, Binzhou University, Binzhou, PR China
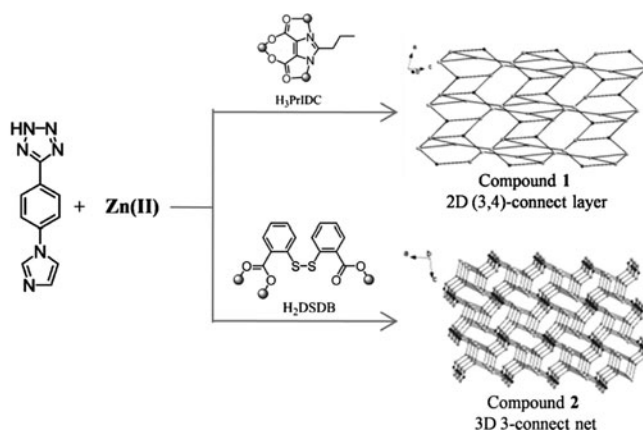
Two Zn(II) coordination polymers with intricate 2-D network and 3-D framework with new 3-connected topology were constructed.

Reactions of Zn(II) salts, 5-(4-(1H-imidazol-1-yl)phenyl)-1H-tetrazolate (HIPT) and 2-mercaptobenzoic acid or 2-propyl-1H-imidazole-4,5-dicarboxylic acid (H_3PrIDC), result in two mixed-ligand coordination polymers (CPs), $[Zn_2(IPT)(DSDB)(OH)]_n$ (H_2DSDB = 2,2′-disulfanediyldibenzoic acid, **1**) and $[Zn_2(IPT)(PrIDC)(H_2O)]_n$ (H_3PrIDC = 2-propyl-1H-imidazole-4,5-dicarboxylic acid, **2**). Compound **1** possesses a 2-D structure built by 1-D $[Zn(IPT)]_n$ chains and $DSDB^{2-}$ connectors, in which the $DSDB^{2-}$ is generated *via in situ* reaction from 2-mercaptobenzoic acid. It displays a new intricate 4-nodal $\{3\cdot4\cdot6\cdot7\cdot8\cdot9\}\{3\cdot6\cdot7\cdot8\cdot9\cdot10\}\{3\cdot8\cdot9\}\{4\cdot6\cdot8\}$ topology. Compound **2** displays a 3-D framework with new 3-connected topology with Schläfli symbol of $(4\cdot8\cdot10)$ $(8\cdot12^2)$, in which the 1-D Zn-carboxylate chains were bridged by 3-connected IPT⁻ ligands. The thermal stabilities and

---

*Corresponding authors. Email: bzuxie@163.com (Y. Xie); hpzeng@scut.edu.cn (H. Zeng)

luminescence properties of **1** and **2** have also been studied. The compounds exhibit intense solid-state fluorescent emissions at room temperature.

1. Introduction

Synthesis of coordination polymers (CPs) has attracted attention for intriguing architectures and applications in adsorption, separation, fluorescence, catalysis, magnetism, etc. [1–3]. Among many factors, the intrinsic nature of ligands has been documented as crucial in construction of CPs. Therefore, it is significant to optimize organic building blocks for desirable structural motifs. Particular attention has been given to tetrazole, which has rich coordination chemistry derived from its flexible coordination modes [4]. Introducing an additional group on the 5-position of tetrazole has been utilized in coordination chemistry of tetrazolyl-based ligand [5–7]. The substituted group on the 5-position can bring steric hindrance to the tetrazole ring or introduce additional weak interaction or coordination sites, which would direct the structures and can yield novel products. Many 5-substituted ligands, such as 5-(pyridyl) tetrazolate [8–10] and 5-(pyrimidyl)tetrazolate [11–14], have been studied extensively. To further explore the coordination chemistry of 5-substituted tetrazole-based ligand, 5-[4-(1H-imidazol-1-yl)phenyl]1H-tetrazolate (HIPT) was selected in this study. The imidazole group that possesses strong coordination ability provides an additional coordination site compared with the parent tetrazole group. Imidazole and tetrazole have similar geometries but seldom are introduced in the same ligand. Only a few CPs based on HIPT were reported [15–22].

Incorporation of more types of metal ions or organic ligands into a single unique framework is worth studying because the functionality of CPs is mainly derived from metal ions and ligands [23, 24]. The combination of nitrogen donor ligands and aromatic carboxylate has been proven to be an effective strategy for constructing diverse mixed-ligand CPs [25, 26]. Some scientists, such as Kim, Hupp, Li, and Chen *et al.*, have succeeded in obtaining several series of functional porous complexes by this strategy. A large number of mixed-ligand pillar-layer CPs constructed by metal-carboxylate layers and nitrogen donor linkers have been constructed by this strategy, and new CPs synthesized via ligand-exchange from this system were also obtained [27–29]. Most of the mixed-ligand CPs use mono-functional N-donor ditopic ligands. Using bifunctional N-donors may have significant influence on the structural type of mixed-ligand CPs and have potential to prepare more CPs compared with mono-functional ligands, but those using bifunctional N-donors are less explored [15].

In this study, we synthesized new CPs based on HIPT and carboxylates as coligands. Two new Zn(II) CPs, $[Zn_2(IPT)(DSDB)(OH)]_n$ (**1**) and $[Zn_2(IPT)(PrIDC)(H_2O)]_n$ (**2**), were synthesized (scheme 1), and their thermal stabilities and luminescence properties have been studied. CPs based on HIPT are still limited [15–22].

2. Experimental

2.1. *Materials and instrumentation*

HIPT was synthesized according to the literature [15]. Thiosalicylic acid was purchased from Aladdin. All other solvents and reagents were obtained from commercial vendors and

used as purchased. Elemental analyses of C, H, and N were measured with a Thermo FlashEA112 elemental analyzer. IR spectra were recorded using a Shimadzu IR Prestige-21 spectrometer with KBr pellets from 4000 to 400 cm^{-1}. X-ray powder diffraction measurements were performed on a Bruker D8 Advance diffractometer at 40 kV, 40 mA with a Cu-target tube and a graphite monochromator. Solid-state fluorescence spectra were measured using a Hitachi-2500 spectrophotometer with a 150-W xenon lamp as light source at room temperature. Thermogravimetric analyses (TGA) were determined with a Netzsch STA409PC Thermal Analyzer from room temperature to 700 °C under air.

2.2. Synthesis of 1 and 2

2.2.1. Syntheses of [Zn$_2$(IPT)(DSDB)(OH)]$_n$ (1). A mixture of HIPT (10.6 mg, 0.05 mmol), Zn(OAc)$_2$·2H$_2$O (10.9 mg, 0.05 mmol), thiosalicylic acid (7.7 mg, 0.05 mmol), and distilled water (6 mL) was sealed in a 10-mL Teflon-lined stainless steel autoclave, and KOH (1 M/L) was used to adjust the pH at 6. The mixture was heated at 180 °C for 3 days under autogenous pressure and cooled at 5 °C h^{-1} to room temperature. Colorless needle-shaped crystals of **1** with gray precipitates were obtained. Yield 15% (based on the Zn). Elemental analysis Calculated (%) for C$_{24}$H$_{15}$N$_6$O$_5$S$_2$Zn$_2$: C, 43.52; H, 2.28; N, 12.69. Found: C, 43.48; H, 2.31; N, 12.68%. IR (KBr, v/cm^{-1}): 3414(m), 3144(m), 2927(w), 2849 (w), 1748(w), 1593(s), 1538(s), 1392(s), 840(m), 741(m), 647(w), 562(w).

2.2.2. Syntheses of [Zn$_2$(IPT)(PrIDC)(H$_2$O)]$_n$ (2). A mixture of HIPT (10.6 mg, 0.05 mmol), Zn(OAc)$_2$·2H$_2$O (10.9 mg, 0.05 mmol), 2-propyl-1 h-imidazole-4,5-dicarboxy-acid (H$_3$PrIDC, 9.9 mg, 0.05 mmol), and distilled water (6 mL) was sealed in a 10-mL Teflon-lined stainless steel autoclave, and HCl (1 M/L) was used to adjust the pH at 3–6. The mixture was heated at 180 °C for 3 days under autogenous pressure and slowly cooled at 2 °C h^{-1} to room temperature. Yellow block-shaped crystals of **2** with gray precipitates were

Scheme 1.   The formation of two mixed-ligand Zn(II) CPs.

obtained. The single crystals could be easily separated from the precipitate by hand, washed with distilled water, and dried in air. Yield 58% (based on the Zn). Elemental analysis Calculated (%) for $C_{18}H_{16}N_8O_5Zn_2$: C, 38.94; H, 2.90; N, 20.18. Found: C, 38.90; H, 2.92; N, 20.20%. IR (KBr, v/cm^{-1}): 3424(w), 3113(s), 2923(w), 2850(w), 2349(s), 1552(s) 1462(m), 1397(s), 1306(s), 1265(s), 1117(m), 1076(m), 969(m), 846(s), 756(m) 658(m), 551(w).

2.3. *X-ray diffraction determination*

Suitable single crystals of **1** and **2** were selected and mounted in air on thin glass fibers. Diffraction data were collected on a Bruker Apex II CCD diffractometer operating at 50 kV and 30 mA using Mo *Kα* radiation ($\lambda = 0.71073$ Å). Multiscan absorption corrections were applied with *SADABS* [30]. The structures were solved by direct methods and refined by full-matrix least squares on F^2 using SHELXL [31]. Anisotropic thermal parameters were used to refine all non-H atoms. Hydrogens were generated geometrically and refined as riding with isotropic thermal factors. A summary of crystallographic and structural refinement data for **1** and **2** is given in table 1. The CCDC reference numbers for **1** and **2** are 965824 and 965826, respectively. Copy of the data can be obtained free of charge on application to CCDC, 12 Union Road, Cambridge CB2 1EZ, UK [Fax: +44 1223 336 033; E-mail: deposit@ccdc.cam.ac.uk].

3. Results and discussion

3.1. *Syntheses and IR spectroscopy*

Because the coordination competition between ligand and coligand may influence formation of mixed-ligand CPs, many experiments with different molar ratios of the metal salt, HIPT and H2DSDB/H3PrIDC, were explored. With a molar ratio of 1 : 1 : 1, 1 : 2 : 1, and 1 : 1 : 2, it was discovered that all of those conditions produce the same products, just with

Table 1.   Crystallographic data and structure refinement summary for **1** and **2**.

Compound	**1**	**2**
Empirical formula	$C_{24}H_{15}N_6O_5S_2Zn_2$	$C_{18}H_{16}N_8O_5Zn_2$
Formula weight	662.28	555.13
Crystal system	Triclinic	Monoclinic
Space group	*P*-1	*C*2/c
a/Å	8.307(9)	21.117(14)
b/Å	12.121(14)	11.270(7)
c/Å	13.297(14)	17.757(17)
α/°	66.544(11)	90
β/°	77.561(13)	100.866(13)
γ/°	89.463(14)	90
V/Å^3	1195(2)	4150(5)
Z	2	2
D/g cm^{-3}	1.841	1.777
μ/mm^{-1}	2.234	2.363
T/K	293(2)	293(2)
R^a/wR^b	0.1261/0.3013	0.0559/0.1319
Total/unique/R_{int}	5453/4060/0.0610	10,459/4058/0.0928

$^a R_1 = \sum ||F_0| - |F_c||/\sum |F_0|.$
$^b wR_2 = \{\sum [w(F_0^2 - F_c^2)^2]/\sum (F_0^2)^2\}^{1/2}.$

different yields, which indicated that stoichiometry factors have less influence on the self-assembly process.

Their IR spectra (figures S1 and S2 [see online supplemental material at http://dx.doi.org/10.1080/00958972.2015.1028383]) show the characteristic absorptions of carboxylate groups from 1593 to 1655 cm^{-1} for asymmetric stretches (ν_{as}) and 1323 to 1423 cm^{-1} for symmetric stretches (ν_s). The absence of strong absorptions around 1710 cm^{-1} for **2** indicates that all carboxyl groups of H3PrIDC ligand are deprotonated.

3.2. *Crystal structure*

Using 2-mercaptobenzoic acid as reactant, we obtained **1**. The X-ray diffraction analyses reveal that 2-mercaptobenzoic was converted to DSDB^{2-} *via in situ* reaction (scheme 2). Compound **1** cannot be obtained using DSDB^{2-} as reactant. Therefore, the *in situ* reaction showed important influence on formation of final product. Such *in situ* reactions have been observed from some ligands containing mercapto group [32, 33]. As shown in figure 1(a), both Zn1 and Zn2 showed distorted tetrahedral geometry with a ZnN$_2$O$_2$ and ZnNO$_3$ coordination, respectively. Zn1 is surrounded by one N$_{tz}$, one N$_{iz}$, one carboxyl O, and one water O, whereas Zn2 is surrounded by one N$_{tz}$, two carboxylate O, and one water O. All the Zn–N and Zn–O bonds are in the normal range [34–36].

The IPT$^-$ exhibited a μ_3-coordination, bridging three Zn(II) ions *via* 1 and 4 nitrogens of the tetrazole group (N$_{tz}$) and one N of imidazole (N$_{im}$). Two IPT$^-$ anions and two Zn(II) ions are joined to form a binuclear ring with Zn–Zn separation of 10.308 Å. Then, the binuclear subunits are further linked by N–Zn–O–Zn coordination sequence, resulting in a 1-D chain extending along the *a* direction [figure 1(b)]. Every two 1-D chains are connected by two DSDB^{2-} anions, giving a 2-D plane [figure 1(c)]. Both Zn1 and Zn2 are four-connected nodes (with point symbol of {3·4·6·7·8·9} and {3·6·7·8·9·10}, respectively) and both IPT$^-$ and DSDB^{2-} are three-connected nodes (with point symbol of {3·8·9} and {4·6·8}, respectively), so the overall topology of **1** is a (3,4)-connected network but with point symbol of {3·4·6·7·8·9}{3·6·7·8·9·10}{3·8·9}-{4·6·8} [figure 1(d)]. The 2-D layers are packed closely *via* the *b* axis to form a 3-D supramolecular framework. No obvious interactions were found between the layers.

Although the coordination mode of IPT$^-$ in **1** is the same as other reported mixed-ligand Zn(II) CPs, [Zn(L)(pbda)$_{0.5}$] (pdba = 1,4-benzenedicarboxylic acid) and [Zn$_{1.5}$(L)(2,5-pydc)] (2,5-pydc = 2,5-pyridinedicarboxylate), the subunit composed of Zn(II) ions and IPT$^-$ anions is quite different. In [Zn(L)(pbda)$_{0.5}$] and [Zn$_{1.5}$(L)(2,5-pydc)], the connection of Zn(II) ions and IPT$^-$ anions lead to a 2-D (4·82) network and (4,4) net with helical chains, respectively; they only connect into binuclear units in **1**. Part of the reason is coordination OH$^-$ in **1**. The coordination OH$^-$ occupies some coordination sites of Zn(II) ions, preventing the formation of higher-dimensional Zn-IPT subunits. In addition, **1** represents the first mixed-ligand CP based on IPT$^-$ and dicarboxylate with a semi-rigid spacer. Because of the semi-rigid character of DSDB^{2-}, two carboxyl groups are confined in the same plane, easier to form a lower-dimensional network in **1** (2-D) compared with the CPs based on Zn(II), IPT$^-$, and rigid dicarboxylate coligand (3-D).

Compound **2** crystallizes in the monoclinic space group *C*2/c. There are two Zn(II) ions, one PrIDC^{3-}, one IPT$^-$, and one coordinated water in the asymmetric unit. As shown in figure 2(a), Zn1 is coordinated by two *N,O*-chelating sites from two different PrIDC^{3-} anions and one N$_{tz}$, resulting in a distorted tetragonal pyramid coordination geometry. Zn2

also adopts distorted tetragonal pyramid coordination geometry with two carboxylate O from PrIDC^{3-}, one N_{tz}, N_{iz}, and one coordinated water. The IPT$^-$ has a μ_3 coordination mode. PrIDC^{3-} displays μ_3-NO,O′O″,O″N′ coordination mode, which is usually found in imidazole-based dicarboxylate ligands [37–39].

The μ_3-coordinated PrIDC^{3-} anions connect Zn(II) ions to a 1-D zigzag chain [figure 2(b)]. Each μ_3-IPT$^-$ ligand connects to three 1-D chains by Zn–N bonds [figure 2(c)], thus the 1-D chains are bridged by μ_3-IPT$^-$ ligands to form a 3-D framework [figure 2(d)]. This structure is condensed partly due to the propyl group on the 2-position of PrIDC^{3-}. To better understand the whole structure of **2**, the topological analysis approach was employed. Every Zn1 connect to two PrIDC^{3-} anions and one IPT$^-$ can be regarded as a 3-connected node, every Zn2 connects to one PrIDC^{3-} and two IPT$^-$ can also be seen as 3-connected nodes. The μ_3-IPT$^-$ and μ_3-coordination PrIDC^{3-} are considered as 3-connected nodes, too. As a result, the Zn1 and μ_3-coordination PrIDC^{3-} possess the same Schläfli symbol of $(8·12^2)$, whereas Zn2 and μ_3-IPT$^-$ ligand possess the same Schläfli symbol of $(4·8·10)$ [figure 2(e)]. Thus the 3-D framework with the Schläfli symbol $(4·8·10)$ $(8·12^2)$ analysis by TOPOS [40] is obtained, which is has not been reported.

Generally, mixed-ligand CPs based on nitrogen donor ligands and aromatic carboxylate divide into three types from a structural standpoint: metal-nitrogen donor ligand subunit plus carboxylate linker (type **I**), metal-carboxylate ligand subunit plus nitrogen donor linker (type **II**), and metal-nitrogen donor ligand subunit plus metal-carboxylate ligand subunit (type **III**). Obviously, **1** belongs to type **I**, and **2** belongs to type **II**. Compared with type **I**, the type **II** structures are less observed in the Zn-IPT-carboxylate system, only including **2** and [Cd(HL)(1,2,4,5-btec)0.5] using 1,2,4,5-benzenetetracarboxylate as coligand.

3.3. *PXRD and TGA*

In order to check the purity of **1** and **2**, the as-isolated samples of **1** and **2** were characterized by powder X-ray diffraction (PXRD) at room temperature (figures S3 and S4). When compared to the simulated patterns generated from single-crystal diffraction data, the measured patterns are in agreement with the calculated diffractograms, indicating that single phases of **1** and **2** are formed. The difference in reflection intensity between the simulated and measured patterns may be attributed to a certain degree of preferred orientation of the powder samples during data collection.

The thermal stabilities of **1** and **2** were examined by TGA under an N_2 atmosphere for crystalline samples from 30 to 800 °C with a heating rate of 10 °C/min. As illustrated in figure 3, **1** showed weight loss gradually from room temperature to 350 °C, which may be due to the part decomposition of DSDB^{2-}. After 350 °C, the framework starts collapsing. For **2**, the TG curve displays a weight loss of 3.8% from room temperature to 125 °C for
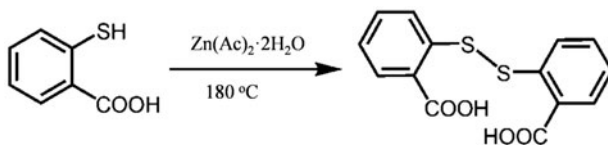
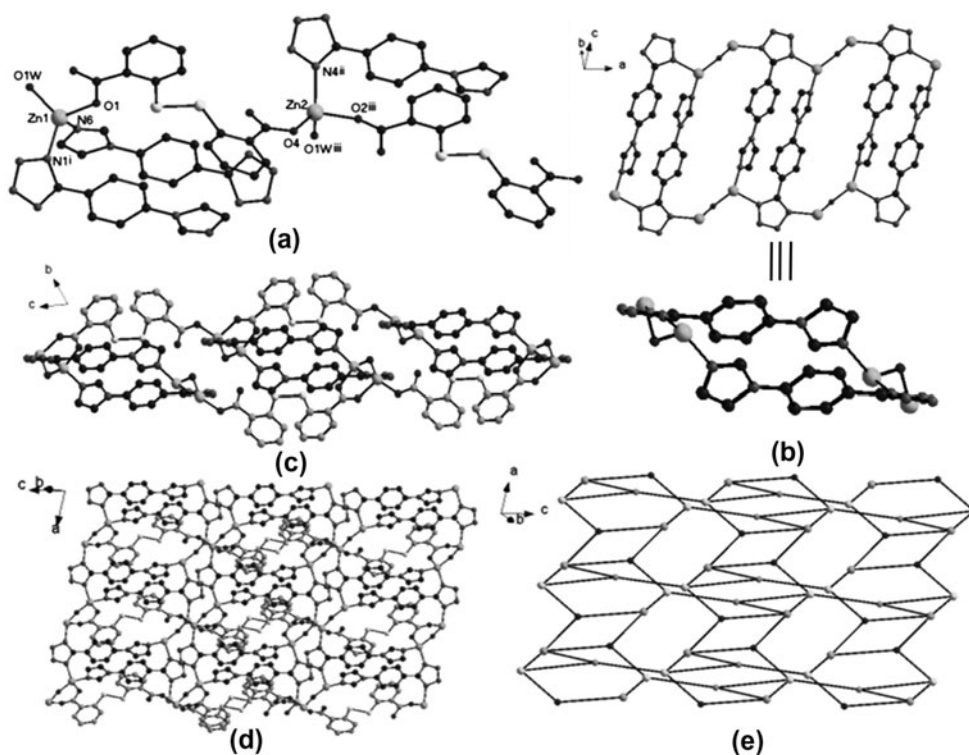Scheme 2.   The *in situ* reaction from 2-mercaptobenzoic acid to H$_2$DSDB.

Figure 1.　(a) Coordination environment of Zn(II) in **1**. (b) Side view and top view of 1D chain based on binuclear rings in **1**. Side view (c) and top view (d) of the 2D layer in **1** (the C atoms on DSDB^{2-} are highlighted in black). (e) The (3,4)-connected topology in **1**.

removal of coordinated water (calculated 3.2%) in the asymmetric unit. The major weight loss occurs in the next step above 430 °C, which may be ascribed to decomposition of the coordination framework.

3.4. *Photoluminescent property*

Taking into account the luminescent properties of d^{10} ions [41, 42], photoluminescence of selected compounds was investigated at room temperature in the solid state. All compounds show much weaker emission intensity compared with HIPT, due to the quenching effect of Zn^{2+}. As illustrated in figure 4, upon photoexcitation, **1** and **2** display maximum emission peaks at 409 (λ_{ex} = 354 nm, figure S5) and 333 (λ_{ex} = 288 nm, figure S6), respectively. Compared with the emissions of HIPT at 362 nm (λ_{ex} = 285 nm) and H$_2$DSDB at 445 nm (λ_{ex} = 384 nm), the emission bands of **1** and **2** can be attributed to H$_2$DSDB-centered and HIPT-centered emissions, respectively. The emission bands of the selected compounds indicate some blue/red shifts, which can be attributed to the coordination of ligands and Zn(II).
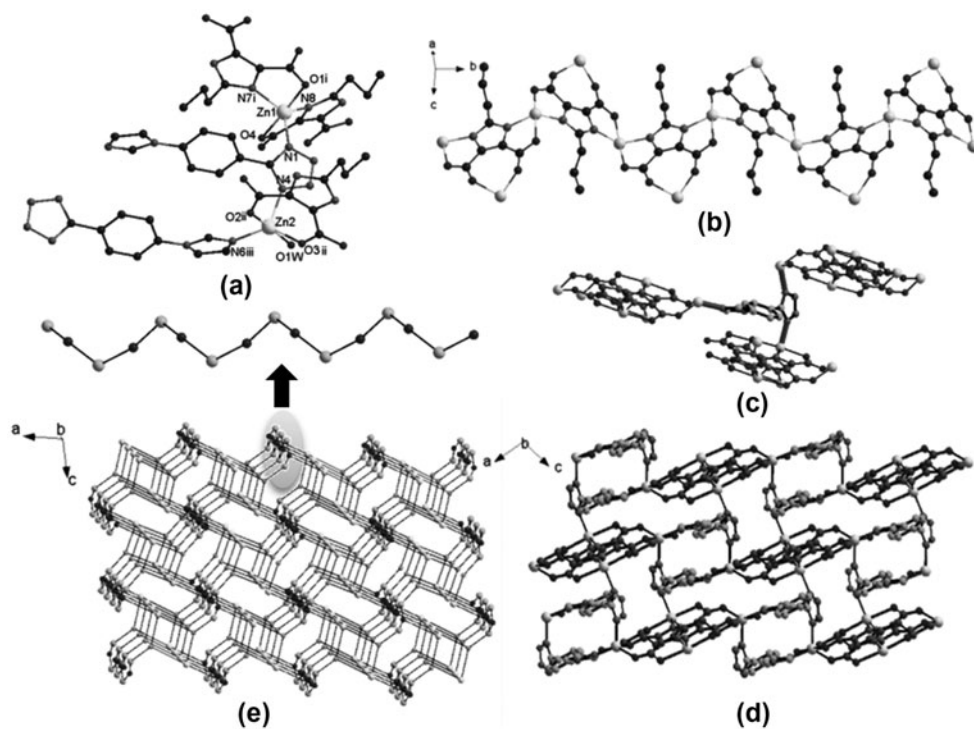
Figure 2. (a) Coordination environment of Zn(II) in **2**. (b) The 1D chain constructed by Zn(II) and PrIDC^{3-} in **2**. (c) Three 1D chains are linked by IPT$^-$ in **2**. (d) The 3D framework in 2 (C atoms on IPT$^-$ are in gray, the C atoms on PrIDC^{3-} are in black). (e) The three-connected topology in **2**.
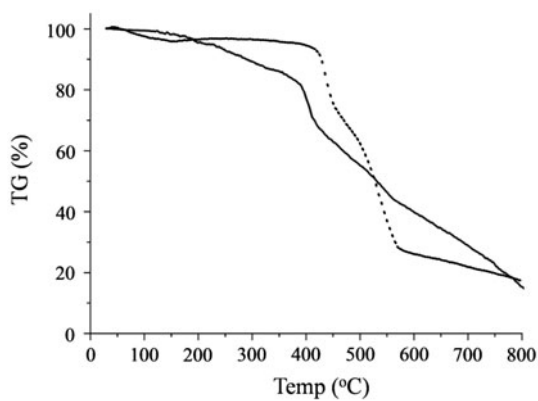

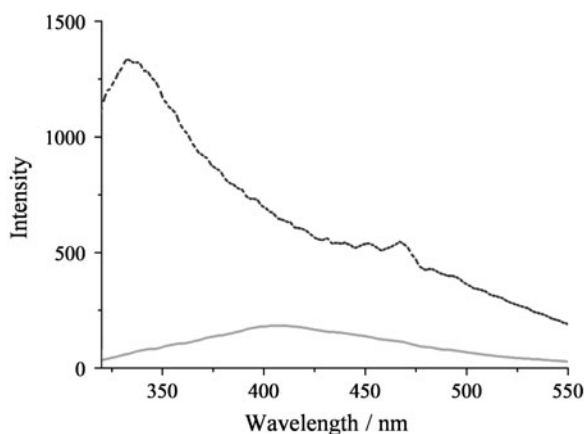Figure 3. TG curve of **1** (solid line) and **2** (dashed line).

Figure 4.   Solid-state photoluminescent spectra of **1** (solid line) and **2** (dashed line) at room temperature.

4. Conclusion

Two new mixed-ligand Zn(II) CPs were constructed based on a bifunctional N-donor ligand and carboxylate coligands. Compound **1** is a new 2-D four-nodal (3,4)-connected network with point symbol of $\{3\cdot4\cdot6\cdot7\cdot8\cdot9\}\{3\cdot6\cdot7\cdot8\cdot9\cdot10\}\{3\cdot8\cdot9\}\{4\cdot6\cdot8\}$. Compound **2** possesses a new 3-connected framework with the Schläfli symbol $(4\cdot8\cdot10)\,(8\cdot12^2)$. This work may be helpful in the construction of mixed-ligand CPs.

Supplementary material

CCDC 965824 and 965826 contain the supplementary crystallographic data for **1** and **2**. These data can be obtained free of charge via http://www.ccdc.cam.ac.uk/conts/retrieving. html, or from the Cambridge Crystallographic Data Center, 12 Union Road, Cambridge CB2 1EZ, UK; Fax: (+44)1223 336 033; or E-mail: deposit@ccdc.cam.ac.uk. Supplementary data associated with this article can be found in the online version.

Disclosure statement

No potential conflict of interest was reported by the authors.

Funding

References

[1] M.D. Allendorf, C.A. Bauer, R.K. Bhakta, R.J.T. Houk. *Chem. Soc. Rev.*, **38**, 1330 (2009).
[2] A. Dhakshinamoorthy, H. Garcia. *Chem. Soc. Rev.*, **41**, 5262 (2012).
[3] Y. Cui, Y. Yue, G. Qian, B. Chen. *Chem. Rev.*, **112**, 1126 (2012).
[4] H. Zhao, Z.R. Qu, H.Y. Ye, R.G. Xiong. *Chem. Soc. Rev.*, **37**, 84 (2008).
[5] M. Dincǎ, J.R. Long. *J. Am. Chem. Soc.*, **129**, 11172 (2007).
[6] F. Nouar, J.F. Eubank, T. Bousquet, L. Wojtas, M.J. Zaworotko, M. Eddaoudi. *J. Am. Chem. Soc.*, **130**, 1833 (2008).
[7] J.R. Li, Y. Tao, Q. Yu, X.H. Bu, H. Sakamoto, S. Kitagawa. *Chem.–Eur. J.*, 14, 2771 (2008).
[8] B.Y. Wu, C.I. Yang, M. Nakano, G.H. Lee. *Dalton Trans.*, **43**, 47 (2014).
[9] X.B. Li, G.M. Zhuang, X. Wang, K. Wang, E.Q. Gao. *Chem. Commun.*, **49**, 1814 (2013).
[10] J.Q. Sha, J.W. Sun, M.T. Li, C. Wang, G.M. Li, P.F. Yan, L.J. Sun. *Dalton Trans.*, **42**, 1667 (2013).
[11] T. Wen, M. Li, X.P. Zhou, D. Li. *Dalton Trans.*, **40**, 5684 (2011).
[12] A. Rodríguez-Diéguez, A. Salinas-Castillo, A. Sironi, J.M. Seco, E. Colacio. *CrystEngComm*, **12**, 1876 (2010).
[13] A.J. Mota, A. Rodríguez-Diéguez, M.A. Palacios, J.M. Herrera, D. Luneau, E. Colacio. *Inorg. Chem.*, **49**, 8986 (2010).
[14] O. Sengupta, P.S. Mukherjee. *Inorg. Chem.*, **49**, 8583 (2010).
[15] S.S. Hou, J.B. Tan, Z.Y. Lian, D.W. Zeng, T.L. Huang, B.R. Huang, S.R. Zheng, J. Fan, W.G. Zhang. *Inorg. Chem. Commun.*, **47**, 112 (2014).
[16] P. Du, Y. Yang, D.W. Kang, J. Yang, Y.Y. Liu, J.F. Ma. *CrystEngComm*, **16**, 6372 (2014).
[17] Z. Shi, J. Peng, X. Yu, Z. Zhang, X. Wang, W. Zhou. *Inorg. Chem. Commun.*, **41**, 84 (2014).
[18] J. Sun, D. Zhang, L. Wang, R. Zhang, J. Wang, Y. Zeng, J. Zhan, J. Xu, Y. Fan. *J. Solid State Chem.*, **206**, 286 (2013).
[19] Z. Shi, Z. Zhang, J. Peng, X. Yu, X. Wang. *CrystEngComm*, **15**, 7199 (2013).
[20] Z. Shi, J. Peng, Z. Zhang, X. Yu, K. Alimaje, X. Wang. *Inorg. Chem. Commun.*, **33**, 105 (2013).
[21] X. Wang, J. Peng, K. Alimaje, Z. Shi. *CrystEngComm*, **14**, 8509 (2012).
[22] H.W. Kuai, X.C. Cheng, X.H. Zhu. *Inorg. Chem. Commun.*, **25**, 43 (2012).
[23] R.L. Chen, X.Y. Chen, S.R. Zheng, J. Fan, W.G. Zhang. *Cryst. Growth Des.*, **13**, 4428 (2013).
[24] S.L. Cai, S.R. Zheng, Z.Z. Wen, J. Fan, W.G. Zhang. *Cryst. Growth Des.*, **12**, 5737 (2012).
[25] R. Kieltyka, P. Englebienne, J. Fakhoury, C. Autexier, N. Moitessier, H.F. Sleiman. *J. Am. Chem. Soc.*, **130**, 10040 (2008).
[26] X. Zhang, L. Hou, B. Liu, L. Cui, Y.Y. Wang, B. Wu. *Cryst. Growth Des.*, **13**, 3177 (2013).
[27] C. Ding, X. Rui, C. Wang, Y. Xie. *CrystEngComm*, **16**, 1010 (2014).
[28] C. Ding, C. Gao, S. Ng, B. Wang, Y. Xie. *Chem. Eur. J.*, **19**, 9961 (2013).
[29] C.X. Ding, F.H. Zeng, J. Ni, B.W. Wang, Y.S. Xie. *Cryst. Growth Des.*, **12**, 2089 (2012).
[30] G.M. Sheldrick. *SADABS, Program for Empirical Absorption Correction of Area Detector Data*, University of Göttingen, Göttingen (1996).
[31] G.M. Sheldrick. *SHELX 97, Program for Crystal Structure Solution and Refinement*, University of Göttingen, Göttingen (1997).
[32] S.M. Humphrey, R.A. Mole, J.M. Rawson, P.T. Wood. *Dalton Trans.*, **11**, 1670 (2004).
[33] H.B. Zhu, S.H. Gou. *Coord. Chem. Rev.*, **255**, 318 (2011).
[34] F.J. Yin, H. Zhao, X.Y. Xu, M. Guo. *J. Coord. Chem.*, **66**, 3199 (2013).
[35] W.B. Chen, Y.X. Qiu, X.M. Lin, M. Yang, H. Yan, F.X. Gao, Z.J. Yang, W. Dong. *J. Coord. Chem.*, **66**, 1700 (2013).
[36] W.D. Song, S.J. Li, S.W. Tong, D.L. Miao, L.L. Ji, J.B. An. *J. Coord. Chem.*, **65**, 3653 (2012).
[37] Q.G. Zhai, R.R. Zeng, S.N. Li, Y.C. Jiang, M.C. Hu. *CrystEngComm*, **15**, 965 (2013).
[38] J.H. Deng, D.C. Zhong, X.Z. Luo, H.J. Liu, T.B. Lu. *Cryst. Growth Des.*, **12**, 4861 (2012).
[39] X. Feng, J. Wang, B. Liu, L. Wang, J. Zhao, S. Ng. *Cryst. Growth Des.*, **12**, 927 (2012).
[40] V.A. Blatov, A.P. Shevchenko. *TOPOS 4.0*, Samara State University, Samara, Russia (1999).
[41] S.R. Zheng, S.L. Cai, J.B. Tan, J. Fan, W.G. Zhang. *CrystEngComm*, **14**, 6241 (2012).
[42] S.L. Cai, M. Pan, S.R. Zheng, J.B. Tan, J. Fan, W.G. Zhang. *CrystEngComm*, **14**, 2308 (2012).